Comparative quantitative 3D whole-brain mapping of Tfr1-enabled and unmodified anti-β-amyloid antibody biodistribution

Authors
Carolina Buizza[1], Micaela Roque[1], Allison Butt[1], Sarah Sterlace[2], Laura Griffin[2], Janell Richardson[2], Urmas Roostalu[1], Henrik H Hansen[1], Yasir Gallero-Salas[1]

[1] Gubra, Hørsholm Kongevej 11B, Hørsholm, Denmark
[2] Taconic Biosciences, Rensselaer, NY

Corresponding author
Carolina Buizza: cbu@gubra.dk

Background & Aim

Efficient delivery of anti-β-amyloid (Aβ) antibodies across the blood–brain barrier (BBB) remains a central challenge in Alzheimer's disease (AD) therapy. Therapeutic Aβ-targeted antibodies engineered for receptor-mediated transcytosis display improved brain exposure and therapeutic efficacy, yet their brain-wide vascular and parenchymal biodistribution has not been comprehensively quantified at cellular resolution. Moreover, their biodistribution in peripheral tissues and distal anatomical regions, such as the hindlimbs, remains largely uncharacterized.

Methods

We used whole-brain 3D light-sheet fluorescence microscopy combined with AI-based image analysis to quantify and compare the biodistribution of two clinically validated anti-Aβ antibodies: one non-BBB-crossing antibody and one BBB-crossing antibody (targeting human transferrin receptor, hTfR), in humanized TfR mice (n = 6 per group).

Brains and hindlimbs were immunolabeled for human IgG to detect antibody localization and Podocalyxin (Podxl)-CD31 to visualize the vascular network. Deep learning–based segmentation enabled whole-brain reconstruction of the vasculature and voxel-wise classification of antibody signal within vascular vs parenchymal compartments. Antibody biodistribution was quantified across all brain regions defined by the Allen Mouse Brain Atlas.

1 Overview of automated sample preparation and light-sheet fluorescence microscopy pipeline

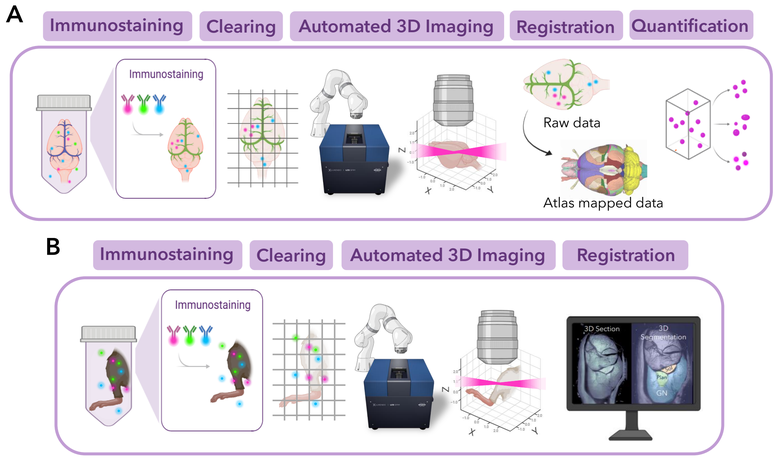

Figure 1. (A) Whole-brain and (B) whole-hindlimb labelling is carried out by immunohistochemistry followed by tissue clearing in ethyl cinnamate (brains) or dibenzyl ether (legs). Custom built robotic systems and light-sheet fluorescence microscopes enable imaging of hundreds of samples at single-cell resolution, generating data for quantitative image analysis.

2 3D whole-brain imaging of therapeutic antibody distribution

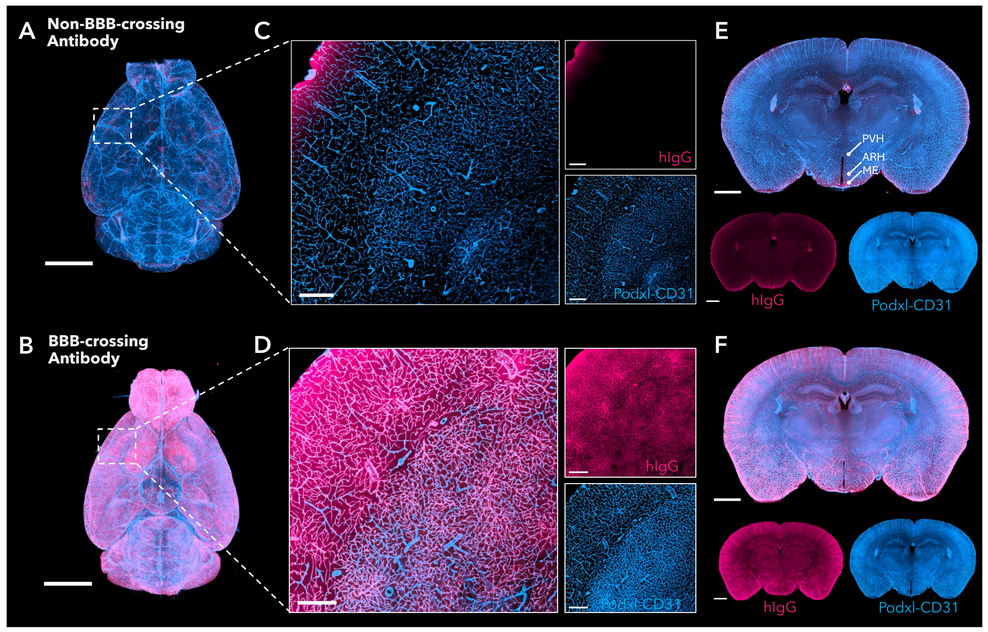

Figure 2. Representative raw data images. Whole-brain samples from hTfrR1 mice were stained for Podxl and CD31 (blue, vasculature) and hIgG (magenta, therapeutic antibodies).
(A-B): representative horizontal 3D brain volumes from mice treated with (A) a non-BBB-crossing antibody and (B) a BBB-crossing antibody (scale bar, 3000 µm).
(C-D): zoomed horizontal 2D maximum intensity projections (80 µm thickness) of cortical regions, highlighting differences in parenchymal and vascular biodistribution for the non-BBB-crossing antibody (C) and the BBB-crossing antibody (D) (scale bar, 300 µm).
(E-F): whole-brain coronal 2D maximum intensity projections (200 µm thickness) from the non-BBB crossing antibody (E) and BBB-crossing antibody (F) (scale bars, 1000 µm).

3 Brain-wide quantification of therapeutic antibody biodistribution in whole-brain, vasculature and parenchyma

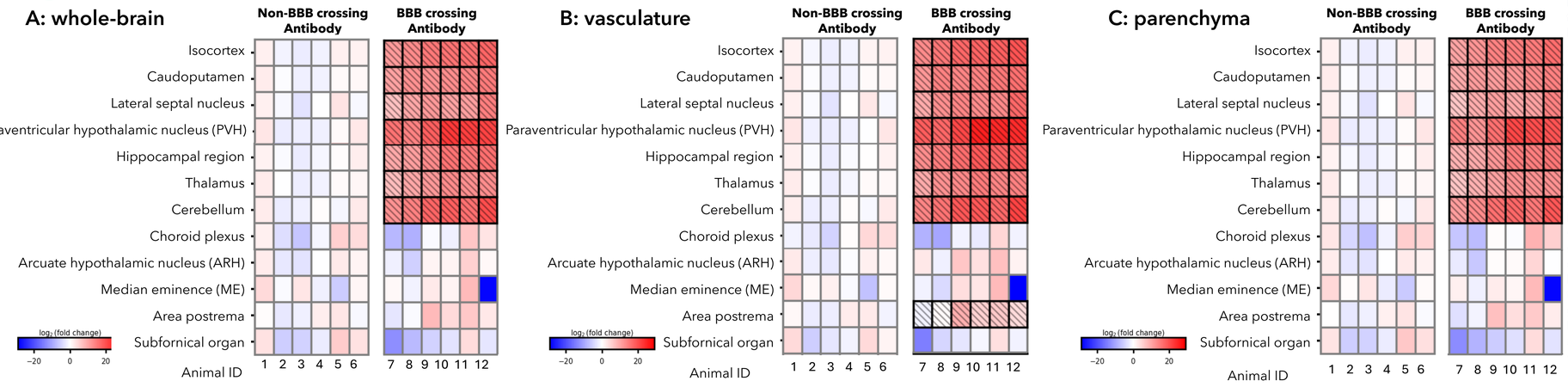

Figure 3. Differences in therapeutic antibody biodistribution profiles across (A) total brain, (B) within vasculature and (C) in the brain parenchyma. Heatmaps show the differences in antibody biodistribution for every animal in the BBB-crossing antibody group compared to the mean value in the Non-BBB crossing antibody group, across 12 selected brain regions. Regions showing statistically significant biodistribution changes are highlighted in hashed and bold. Dunnett's test negative binomial generalized linear model. False discovery rate was applied to correct the p-value.

4 3D whole-hindleg imaging of therapeutic antibody distribution

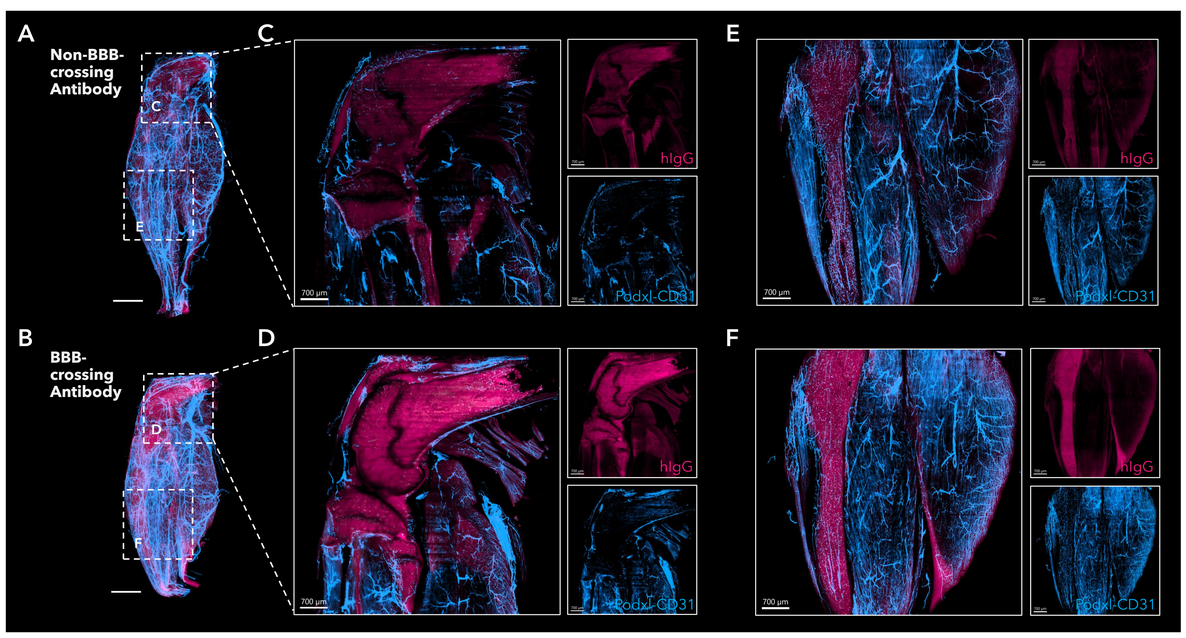

Figure 4. Representative raw data images. Whole-hindlimb samples from hTfrR1 mice were stained for Podxl and CD31 (blue, vasculature) and hIgG (magenta, therapeutic antibodies).
(A-B): representative 3D hindleg volumes from mice treated with (A) a non-BBB-crossing antibody and (B) a BBB-crossing antibody (scale bar, 2000 µm).
(C-D): zoomed 2D maximum intensity projections (200 µm thickness) of the knee, highlighting differences in bone marrow biodistribution for the non-BBB-crossing antibody (C) and the BBB-crossing antibody (D) (scale bar, 700 µm).
(E-F): zoomed 2D maximum intensity projections (200 µm thickness) of the tibia, highlighting differences in bone marrow, muscles and other peripheral tissues biodistribution for the non-BBB-crossing antibody (C) and the BBB-crossing antibody (D) (scale bar, 700 µm).

Conclusion

- Treatment of hTfrR1 mice with a BBB-crossing therapeutical antibody, compared to a non-BBB-crossing control antibody, revealed clear differences in whole-brain and hindlimb biodistribution, as observed in both 3D and 2D imaging datasets.
- In the brain, differences in therapeutical antibody biodistribution were quantitatively assessed across whole-brain, vascular, and parenchymal compartments.
  - Across all three compartiments, the BBB-crossing antibody showed increased biodistribution in multiple brain regions, including the hippocampus, isocortex, thalamus, cerebellum and several additional areas.
- hIgG signal did not differ between treatment groups in regions corresponding to the circumventricular organs, suggesting that enhanced brain distribution of the BBB-crossing antibody is not driven by retention within these naturally permeable regions, but rather reflects transport from the vasculature into the brain parenchyma.
- In the hindlimbs, both the BBB-crossing and non-BBB-crossing antibodies were detected in bone marrow, muscle, and other peripheral tissues. However, the BBB-crossing therapeutical antibody exhibited visually stronger accumulation across these tissues.

Scan the QR code to read more about the BBB and see our videos

www.gubra.dk

PO-1466-EN-2608